

# Dynamic Image Display and Adjustment Method for Glassless 3D Viewing Systems

Isao Nishihara, Takayuki Nakata  
 Department of Information Systems Engineering, Faculty of Engineering  
 Toyama Prefectural University  
 Imizu city, Toyama, Japan

Abstract— In this paper, we propose a simple dynamic image position adjustment method for high-resolution displays in glassless three-dimensional (3D) viewing systems. Glassless stereoscopic displays are currently used in many fields; however, accurately adjusting their physical display position is difficult, especially given their large display area. Our proposed method effects a dynamic adjustment of the positions of images on the display to match various physical conditions in 3D displays. We constructed a simple 3D viewing system using a high-resolution display and a lenticular lens as a prototype. Experimental results confirmed that our method can automatically adjust the positions of images in 3D displays. In future research, we intend to implement this automatic adjustment system.

Keywords-component; Glassless 3D viewing systems; Autostereoscopy; High-resolution display; Lenticular lens; Software adjustment.

## I. INTRODUCTION

Glassless stereoscopic displays have researched for a hundred years[1]-[4], and become popular in recent times[5]. However, accurate adjustment of the position of the physical display for three-dimensional (3D) viewing remains challenging in these systems, especially in large displays. In this paper, we propose a method that dynamically adjusts image position on displays in order to match various physical conditions in 3D displays. In general, when the position of the image is not adjusted, the left and right images are alternately displayed diagonally to each other, and stereoscopic viewing is hence not implemented. When the position of each image is adjusted in the sub-pixels through software processing, the left and right images are uniformly displayed, and stereoscopic viewing becomes possible. Using this method, 3D viewing systems can be installed easily because precise physical alignment is not required. We constructed a simple stereoscopic system using a high-resolution display and a lenticular lens, and confirmed the effectiveness of our method for automatic image position adjustment through experiments.

## II. THEOREM OF ADJUSTMENT SYSTEM IN GLASSLESS 3D VIEWING SYSTEM

In glassless 3D liquid crystal displays, it is necessary to determine the values of parameters  $L$ ,  $P$ ,  $\theta$ , and  $P_h$  in order to accurately adjust the lenticular lens. Each parameter is as follows:

- i. Lines Per Inch (LPI) of lenticular lens:  $L$
- ii. Pixel size of a display:  $P$
- iii. Angle of the lenticular lens to a display:  $\theta$
- iv. Position shift of lenticular lens and the display (initial phase):  $P_h$

The relation among parameters  $L$ ,  $P$ ,  $\theta$ ,  $P_h$ , the lenticular lens, and the display is shown in Figures 1 and 2. The figures contain a front view and a cross-section view, respectively.

In this paper, the frequency  $f$  of the lenticular lines in the horizontal resolution of the display (in the case of a 4K display, 3,840 pixels) is calculated using Equation 1, from the values of  $L$  and  $P$ :

$$L_\theta = \frac{L}{\cos \theta}, f = L_\theta P \frac{3840}{25.4} \quad (1)$$

Lenticular lens and display

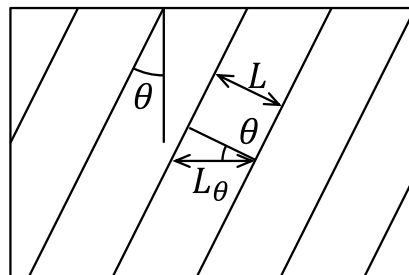


Figure 1. Relation between a lenticular lens and a display (front view)

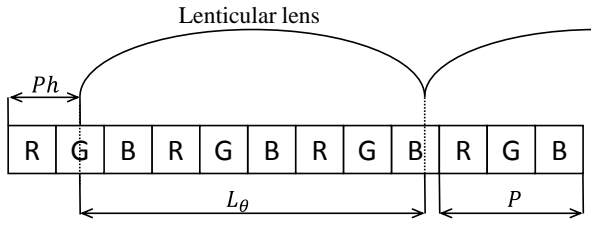


Figure 2. Relation between a lenticular lens and a display  
(cross section view)

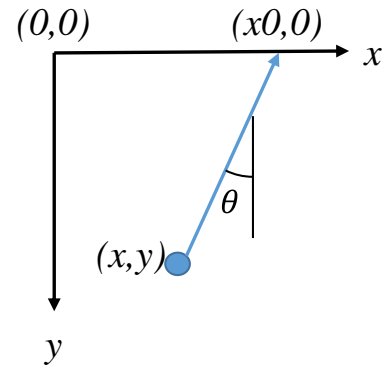


Figure 4. Display calculation method

If  $\theta$  and  $P_h$  can be calculated correctly, the correspondence at the relevant sub-pixel between the display and the angle of the output ray on the lenticular lens can also be correctly calculated. The preconditions of our experimental setup were as follows.

1. Display pixels were horizontally and vertically arranged at the correct regular intervals.
2. The lenticular lenses have exactly parallel, straight edges, and regular intervals.
3. The pixel size of display  $P$ , the LPI of the lenticular lens  $L$ , and the angle between the lenticular lens and the display  $\theta$  were already known to contain errors in the range of approximately 5%.

### III. PROPOSED ADJUSTMENT SYSTEM

Figure 3 shows the overall view of our proposed image adjustment system. We place a USB camera at the observer's position in the system, as shown in the figure. The image captured by the camera is the observed image that is processed, and various parameters are adjusted according to the results of processing.

First, the calculation for drawing the images is shown in Figure 4.

$$x_0 = x + y \tan \theta$$

$$s_0 = (x_0 - P_h) \bmod L_\theta$$

In this method, a line with a width of one sub-pixel is drawn, as shown in Figure 5. The sub-pixels in the following formula are emitted.

$$P_l \leq s_0 < P_l + 1/3$$

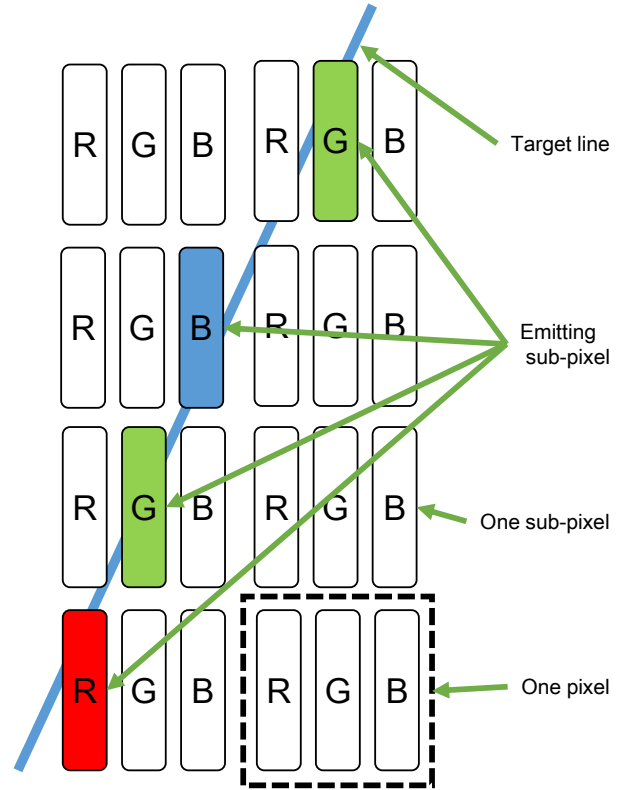


Figure 5. One-sub-pixel horizontal bold line

In this formula,  $1/3$  signifies the size of the sub-pixel and  $P_l$  is the offset of the line in the lens. The displayed image has a simple line with the specified angle  $\theta$  and a one-sub-pixel horizontal bold line, as shown in Figure 5. As shown in the figure, only one sub-pixel in each horizontal line is emitting.

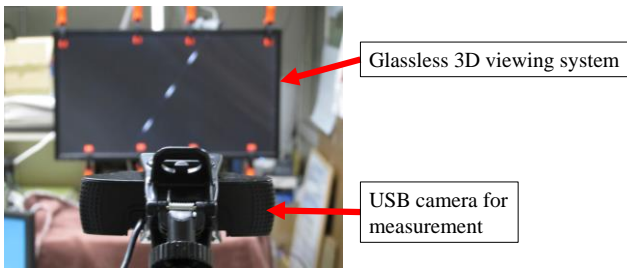


Figure 3. Proposed adjustment system

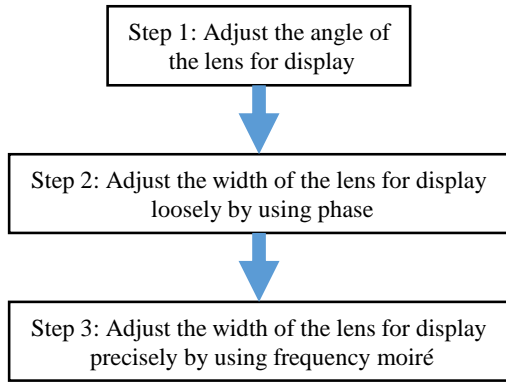


Figure 6. Flowchart of the adjustment system

A flowchart of the adjustment is shown in Figure 6. We first measure angle  $\theta$  between the lens and the display, followed by width  $L_\theta$  of the lens on the display. We use two methods for the latter measurement because the first method using phase has no local solution, whereas the second method using moiré exactly measures the parameters. The second method uses a moiré pattern, and hence a local solution is found at the position in the image divisible by an integer fraction.

The details of each step are as follows.

A. Angle adjustment (Step 1)

Step 1 of our method involves adjustment of the angle of drawing line to the angle of the lenticular lens. Figures 7(a) and (b) show the displayed image and the observed image, respectively, from the USB camera. (For clarity, the lines in Figure 7 are thicker than in the actual image.)

In Step 1, drawing offset  $P_l$  is set to be the center of the display, and  $L_\theta$  is set to an infinite value. This means that only one line is drawn in the display.

The observed image contains a dotted line because the lenticular lens divides the lines, as shown in Figure 7(b). The observed image is processed using the maximum value in all pixels on each horizontal line shown in Figure 8, and the vertical finite list  $f_v(x)$  is calculated. The frequency value with the largest spectral component is then measured. (See Appendix for the method used to obtain frequency in point units.)

We performed measurements by changing angle  $\theta$  in the range  $\pm 5$  degrees in the vicinity of the value expected from the specifications.

An example of the result obtained is shown in Figure 9. In this graph, two lines appear. After the left side of the line is

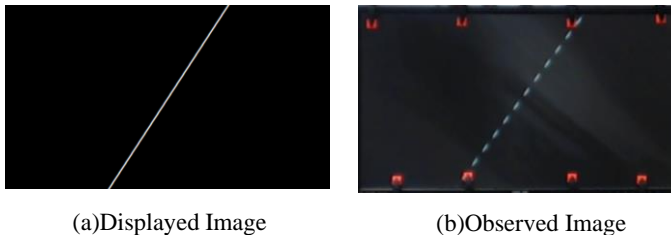


Figure 7. Images in adjusting angle

reversed, then one line is shown in Figure 10. This line appears to be straight, but is actually slightly bent theoretically, with trigonometric functions. Therefore, we applied a second-order approximation formula. The intersection of the x-axis has been

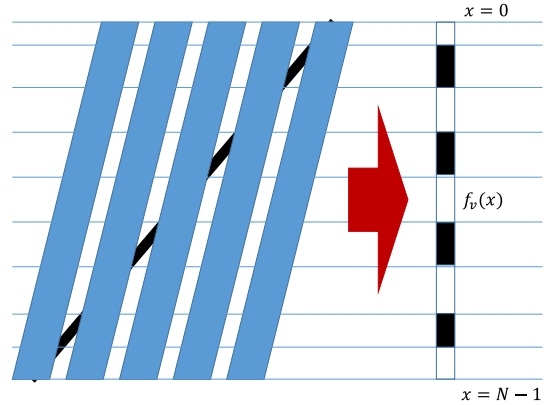


Figure 8. Frequency along vertical lines

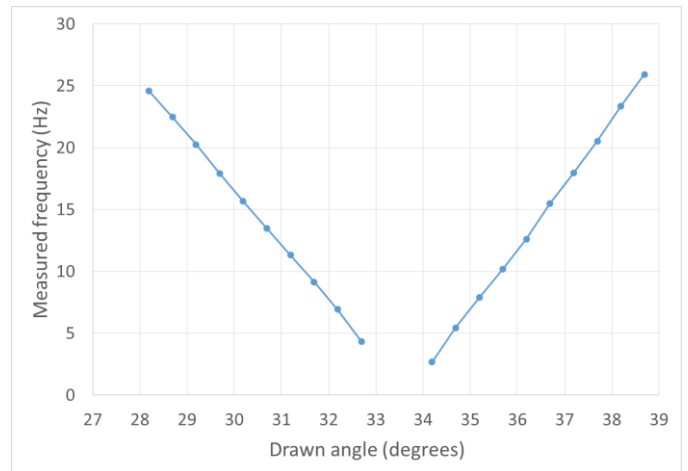


Figure 9. Measured frequency graph

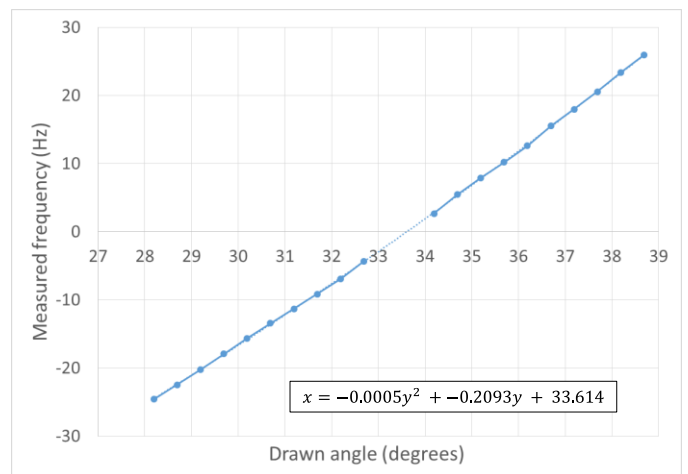


Figure 10. Measured frequency with approximation formula

determined. Hence, the adjusted angle  $\theta_{adj}$  was 33.614 degrees.

**B. Loosely adjusting the width (Step 2)**

Step 2 of our procedure involves a loose adjustment of the width,  $L_\theta$ . This method is similar to Step 1. Different points from Step 1 change the offset of the drawing line instead of the angle, and measure the phase  $\vartheta$  of  $f_v(x)$  instead of frequency (see Appendix).

An example result is shown in Figure 11. In the graph in the figure, a straight line appears. One approximate line was calculated, and the slope S of the line,  $\vartheta$ , was 12.622. The loose width  $w_{adj1}$  was then calculated using Equation 3:

$$w_{adj1} = \frac{360}{|S|} \times 3 \quad (3)$$

In the above equation, the multiplication by three represents the conversion from pixel to sub-pixel level, such as RGB. In this case,  $w_{adj1}$  was 28.521 sub-pixels, and frequency  $f_{adj1}$  was 403.91 Hz in 3,840 pixels.

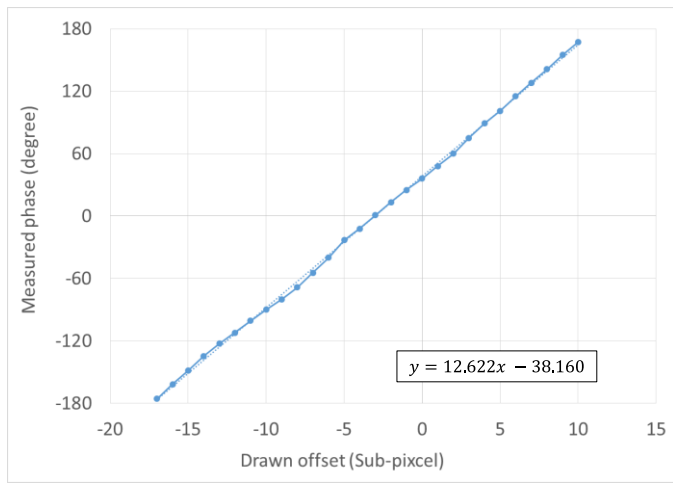


Figure 11. Measured phase graph

**C. Precise adjustment of width (Step 3)**

Step 3 involves precise adjustment of the width  $L_\theta$  by using a moiré pattern. Many lines are drawn in the display image. These lines all have the same angle  $\theta_{adj}$ , the same one-sub-pixel horizontal bold, and the same horizontal interval with changing parameter  $L_\theta$ .

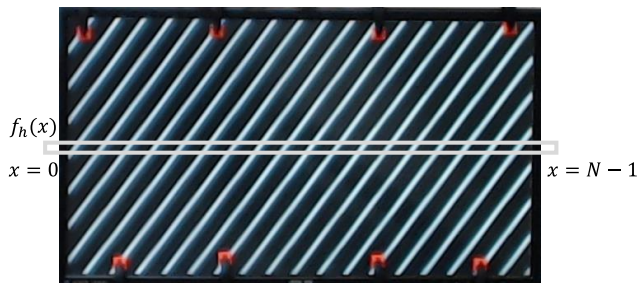


Figure 12. Observed image in Step 3

In this situation, the observed image is shown in Figure 12. The frequency pattern having a value of the difference between the true frequency is observed by moiré. The horizontal finite list  $f_h(x)$  picked up values from pixels on the horizontal line. The frequency with the largest spectral component in  $f_h(x)$  was then measured (see Appendix).

Measurement was performed by changing the drawing frequency in the range  $\pm 50$  Hz around  $f_{adj1}$ . An example result is shown in Figure 13. In this graph, two lines appeared as in Step 1. Further, as in Step 1, the left side of the line is reversed, then one line is shown in Figure 14.

Theoretically, this line is straight. Therefore, we applied the straight line approximation and the intersection with the x-axis was determined. Hence, the adjusted frequency,  $f_{adj2}$ , was 405.18 Hz.

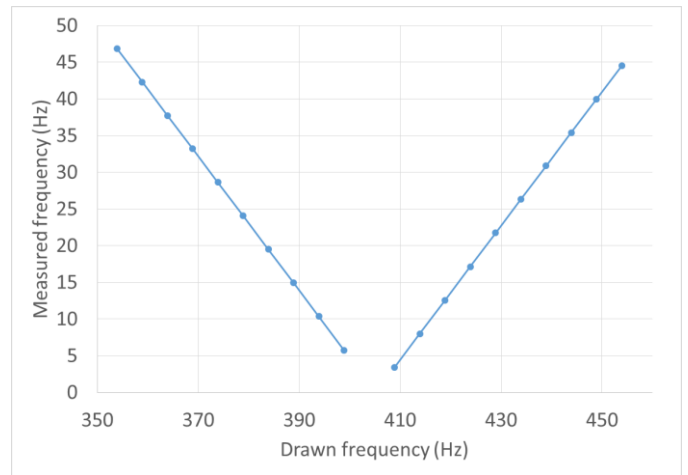


Figure 13. Measured frequency graph

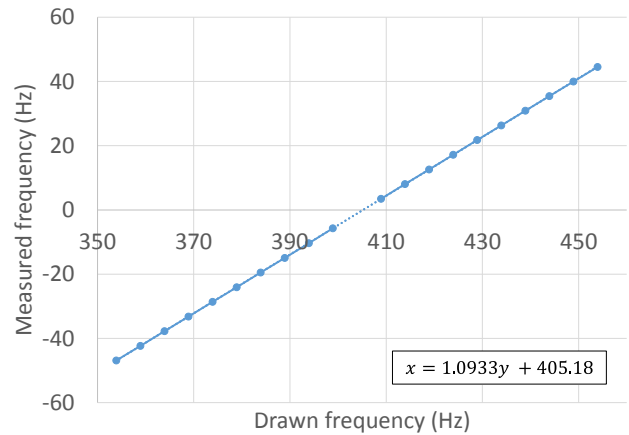


Figure 14. Measured frequency with approximation formula

**IV. EXPERIMENT**

Table I shows the specifications used in our experiment to verify the effectiveness of our proposed method.

From these specifications, we calculated angle  $\theta$  as 33.690 degrees and frequency  $f$  as 404.75 Hz (28.462 sub-pixels).

However, the values were slightly different from the true values for 3D viewing, such as those shown in Figure 15(a). In this figure, the blue image represents the image for the left eye, and the red image represents the image for the right eye. Ideally, separate images are visible for the left eye and the right eye for 3D viewing. However, Figure 15(a) shows how both images appeared to one eye.

Following adjustments, angle  $\theta$  was 33.614 degrees and frequency  $f$  was 405.18 Hz ( $w$  was 28.431 sub-pixels). With these parameters, observers could see only the red image, for the right eye, as shown in Figure 15(b). This situation implies that the observers could see the 3D view.

TABLE I. THE SPECIFICATIONS OF OUR EXPERIMENT

LCD Display	Size	Wide 28 Inches
ASUS PB287Q	Resolution	3,840 × 2,160 Pixels
	Pixel pitch	0.16mm
Lenticular lens	Size	622 × 343 × 3.81 mm
	Lens pitch	20.11 ± 0.02 LPI
Micro Lens Technology, nc.	Cant angle	33.690°

V. CONCLUSION

In this paper, we proposed a simple method to adjust parameters in 3D viewing systems. We confirmed that 3D images appear to be cleaner and clearer using this approach.

In future research, we intend to implement the automatic adjustment system on large 3D display devices. Further, the proposed method will be applied to 3D-interactive systems [6] with large 3D displays [7].

REFERENCES

[1] C.Wheatstone, "Contributions to the Physiology of Vision. -Part the First. On Some Remarkable, and Hitherto Unobserved, Phenomena of Binocular Vision," Philosophical Transactions of Royal Society of London, 128, pp.371-394 (1838).

[2] F.E.Ives, "Parallax Stereogram and Process for Making Same," U.S. Patent Number 725567 (1903).  
 [3] C.W.Kanolt, "Photographic Method and Apparatus," U.S. Patent Number 1260682 (1918).  
 [4] G.M.Lippmann, "Epreuves Reversibles Donnant la Sensation du Relief," J. de Phys. 7, pp.821-825 (1908).  
 [5] Y. Takaki, "Thin-type Natural Three-dimensional Display with 72 Directional Images," Proc. SPIE, 5664, Stereoscopic Displays and Virtual Reality Systems XII (San Jose, CA, USA), 56-63 (2005).  
 [6] I. Nishihara, "Real-time Virtual Three-dimensional Interactive System Using a Stereo Camera," International Workshop on Advanced Image Technology (IWAIT 2014), Virtual Reality 142, B1, 70-73 (2014).  
 [7] I. Nishihara and T. Nakata, "Simple Dynamic Image Adjustment Method for Glassless 3D Viewing Systems, ICAI2015 T107-03, PS1441 (2015).

APPENDIX

In this paper, we conducted frequency and phase detection with real values using discrete Fourier transform (DFT). We show how to calculate frequency using DFT below because it is generally used to measure the integer value. In general, the DFT is represented by the following formula:

$$F(t) = \sum_{x=0}^{N-1} f(x)e^{-i\frac{2\pi tx}{N}}$$

where  $f(x)$  is the value of  $x$  in each pixel, and  $x$  is an integer value. ( $x = 0, \dots, N - 1$ )

For ease of understanding, we change  $F(t)$  to vector  $P$ :

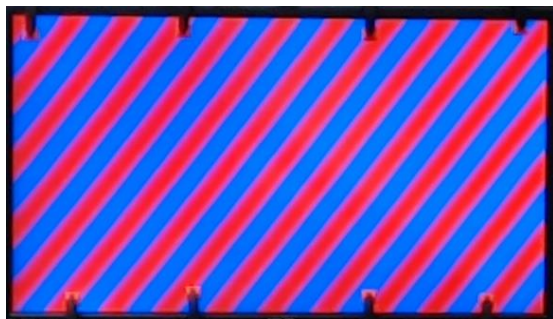
$$P \equiv \left( \sum_{x=0}^{N-1} f(x) \cos\left(\frac{2\pi tx}{N}\right), \sum_{x=0}^{N-1} f(x) \sin\left(\frac{2\pi tx}{N}\right) \right)$$

Then, frequency  $t_{max}$ , which has the largest spectrum, is calculated as

$$t_{max} = t \text{ (when } |P| \text{ has max value)}$$

$$|P| = \sqrt{\left(\sum_{x=0}^{N-1} f(x) \cos\left(\frac{2\pi tx}{N}\right)\right)^2 + \left(\sum_{x=0}^{N-1} f(x) \sin\left(\frac{2\pi tx}{N}\right)\right)^2}$$

$t$  is typically an integer value, but we want the frequency value to be a real value. Hence,  $t$  is changed by 0.001 units, for example, following which all  $|P|$  are calculated for every  $t$ .  $t_{max}$  is chosen when  $|P|$  has the maximum value.



(a)Before adjustment



(b)After adjustment

Figure 15. Final result

Finally, phase  $\vartheta_{max}$  is calculated as follows:

$$\vartheta_{max} = \arg P \text{ (at } t = t_{max}\text{)}$$

#### AUTHORS PROFILE

Isao Nishihara received his B.E., M.E., and Ph.D. degrees in Physical Information Engineering from Tokyo Institute of Technology in 1995, 1997, and 2000 respectively. He is now the assistant professor in the Faculty of Engineering, at Toyama Prefectural University in Japan. His research interests

include digital video image processing, human interfaces, and virtual 3D world.

Takayuki Nakata received his B.E., M.E., and Ph.D. degrees from Kanazawa University in 1998, 2001 and 2004 respectively. From 2002-2004 he was a special research student in Yokohama National University. In 2004, he joined the Faculty of Engineering, Toyama Prefectural University, where he is currently an associate professor. His research interests include recognition of 3D object, 3D display, etc.